BIOCHEMISTRY
including biophysical chemistry & molecular biology

Article

pubs.acs.org/biochemistry

Effect of pH, Temperature, and Salt on the Stability of *Escherichia coli*- and Chinese Hamster Ovary Cell-Derived IgG1 Fc

Cynthia H. Li,*[,†] Linda O. Narhi,[†] Jie Wen,[†] Mariana Dimitrova,[∥] Zai-qing Wen,[‡] Jenny Li,[†] Joseph Pollastrini,[‡] Xichdao Nguyen,[†] Trace Tsuruda,[§] and Yijia Jiang*[,†]

[†]Product Attribute Sciences, Amgen Inc., One Amgen Center Drive, Thousand Oaks, California 91320, United States
[‡]Drug Product Development, Amgen Inc., One Amgen Center Drive, Thousand Oaks, California 91320, United States
[§]Protein Technologies, Amgen Inc., One Amgen Center Drive, Thousand Oaks, California 91320, United States
[∥]Formulation Sciences, Medimmune, One Medimmune Way, Gaithersburg, Maryland 20878, United States

Supporting Information

ABSTRACT: The circulation half-life of a potential therapeutic can be increased by fusing the molecule of interest (an active peptide, the extracellular domain of a receptor, an enzyme, etc.) to the Fc fragment of a monoclonal antibody. For the fusion protein to be a successful therapeutic, it must be stable to process and long-term storage conditions, as well as to physiological conditions. The stability of the Fc used is critical for obtaining a successful therapeutic protein. The effects of pH, temperature, and salt on the stabilities of *Escherichia coli*- and Chinese hamster ovary cell (CHO)-derived IgG1 Fc high-order structure were probed using a variety of biophysical techniques. Fc molecules derived from both *E. coli* and CHO were compared. The IgG1 Fc molecules from both sources (glycosylated and aglycosylated) are folded at neutral pH and behave similarly upon heat- and low pH-induced unfolding. The unfolding of both IgG1 Fc molecules occurs via a multistep unfolding process, with the tertiary structure and C_H2 domain unfolding first, followed by changes in the secondary structure and C_H3 domain. The acid-induced unfolding of IgG1 Fc molecules is only partially reversible, with the formation of high-molecular weight species. The CHO-derived Fc protein (glycosylated) is more compact (smaller hydrodynamic radius) than the *E. coli*-derived protein (aglycosylated) at neutral pH. Unfolding is dependent on pH and salt concentration. The glycosylated C_H2 domain melts at a temperature 4−5 °C higher than that of the aglycosylated domain, and the low-pH-induced unfolding of the glycosylated Fc molecule occurs at a pH ∼0.5 pH unit lower than that of the aglycosylated protein. The difference observed between *E. coli*- and CHO-derived Fc molecules primarily involves the C_H2 domain, where the glycosylation of the Fc resides.

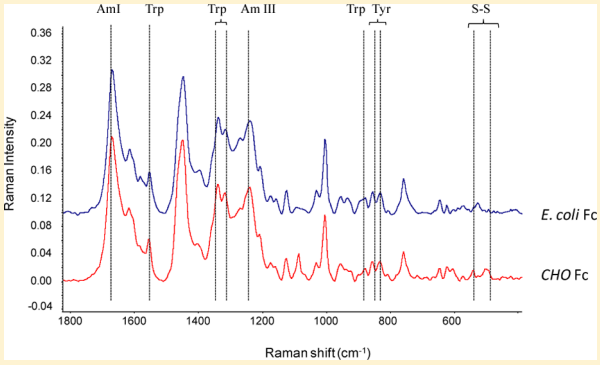

The development of a successful therapeutic is dependent on the fate of the molecule in vivo, in addition to its biological activity. Many molecules with therapeutic potential, such as small peptides, extracellular receptor domains, ligands, or enzymes, are degraded and cleared in the body within minutes.[1,2] The Fc region (Fc) of immunogloblin G1 (IgG1) contains the second (C_H2) and third (C_H3) constant regions of the heavy chain of an IgG1 mAb with one glycosylation site on each C_H2 polypeptide chain and can be used as a scaffolding to prolong the half-life of active peptides and other protein moieties of therapeutic interest. The Fc fusion proteins can be constructed as a single gene that encodes both the Fc and the active therapeutic portion and can be expressed in many cell lines, including *Escherichia coli* or Chinese hamster ovary cells (CHO); the resulting molecule will be glycosylated or aglycosylated depending on the cell line used. Recently, there has been an increased level of interest in the use of Fc fusion proteins because of their attractive characteristics, including the ease of expression and purification and the prolonged half-life they confer. They have become an important class of therapeutic agents, with five drugs, Enbrel, Amevive, Orencia, Arcalyst, and Nplate, currently on the market and many more in various stages of clinical trials.[3]

The conformational stability of the fusion protein depends at least in part on the stability of the IgG1 Fc molecule itself. For an IgG antibody molecule, the carbohydrate appears to play a crucial role in the effector functions of the protein[4,5] and in the clearance pathways available to it. Previous work has shown that the folding and unfolding of an IgG molecule proceed through intermediates, with the domains acting independently.[6−19] In this work, we studied the stability of the IgG1 Fc protein expressed and isolated from *E. coli* (refolded and aglycosylated) or CHO (secreted, folded, and glycosylated) to pH- and heat-induced denaturation and in buffers with

Received: May 30, 2012
Revised: October 15, 2012
Published: October 18, 2012

increasing sodium chloride concentrations to improve our understanding of the effect of pH, heat, and salt on the stability of these IgG1 Fc molecules.

MATERIALS AND METHODS

Materials. The *E. coli*- and CHO-derived Fc molecules were supplied by the Protein Sciences Department at Amgen. The *E. coli*-derived Fc molecule was isolated and refolded from inclusion bodies. Refolding occurred in aqueous buffer with dichlorodiphenyltrichloroethane (DDT) under ambient conditions for 72 h. A two-column chromatography scheme was employed for purification using Bio-Rad Ceramic Hydroxyapatite type I followed by Toso Haas Butyl 650M, with elution at pH ≥4. The resulting Butyl pool was then concentrated and buffer exchanged into PBS. The CHO-derived Fc molecule was purified from CHO-conditioned medium containing human IgG1 Fc molecule. The conditioned medium was harvested every 7 days and filtered through a 0.45 μm cellulose acetate filter (Corning) prior to purification and affinity-purified by using Protein A resin. The protein was eluted with 0.1 M sodium acetate (pH 3.4), immediately neutralized, and then buffer-exchanged into phosphate-buffered saline (PBS). Both purified proteins were >95% pure by reduced and nonreduced sodium dodecyl sulfate−polyacrylamide gel electrophoresis (SDS−PAGE) and/or size exclusion chromatography. Both purified proteins had the same disulfide configuration demonstrated by nonreduced peptide mapping.

For the pH-dependent conformational and thermal stability studies, the *E. coli*-derived Fc molecule at 24.7 mg/mL in PBS was diluted to 3.2 mg/mL with PBS. This made it equivalent to the CHO-derived Fc material that was obtained at 3.2 mg/mL in PBS. Further dilutions of both PBS stock protein solutions were conducted in 20 mM sodium citrate/140 mM sodium chloride (NaCl) buffer at pH 2−7 (C*x*N, where *x* is the pH) or into 20 mM Tris/140 mM NaCl buffer at pH 7−10 (T*x*N, where *x* is the pH) to a final protein concentration of ∼0.5 mg/mL. To evaluate the effect of salt concentration on the conformation and stability of the Fc molecules, the stock solution of the protein was diluted into 20 mM sodium citrate at pH 7, 5, or 3 with 0, 140, 250, 500, or 1000 mM NaCl to a final protein concentration of ∼0.5 mg/mL. The protein solutions were further diluted or concentrated to the concentrations appropriate to the techniques, described in the individual methods sections below. The reversibility was assessed by analysis of the protein that had been incubated at pH 3, 3.5, or 7 in C*x*N buffer for 2 h at room temperature, followed by dialysis into PBS overnight at 4 °C.

Methods. Changes in the conformation and stability of the IgG1 Fc molecules were analyzed using several different techniques. The thermal stability was probed with differential scanning calorimetry (DSC). The hydrodynamic radius was probed with dynamic light scattering (DLS). The size distribution and heterogeneity of each sample were analyzed by field flow fractionation (FFF) and cation exchange chromatography (CEX). The tertiary structure was assessed by near-UV circular dichroism (CD), fluorescence, and Fourier transform Raman (FT-Raman) spectroscopies. The surface hydrophobicity was analyzed using 1,8-anilinonaphthalene sulfonate (ANS) binding. The secondary structure was analyzed with far-UV CD, Fourier transform infrared (FTIR), and FT-Raman spectroscopies.

The similarity between any two spectra and/or profiles was obtained using the Thermo Electron OMNIC software QC compare function. The QC compare function correlates the spectral information in the specified region of the sample and the reference spectra to determine the similarity between the two spectra. The pH 7 spectrum in 20 mM sodium citrate/140 mM NaCl buffer was used as a reference spectrum for all spectral similarity analyses from pH 2 to 7, and the pH 7 spectrum in 20 mM Tris/140 mM NaCl buffer was used as a reference spectrum for all spectral similarity analyses from pH 7 to 10 to avoid the possible differences caused by buffer interference. The reference spectral similarity is always set as 100%. The result is a value between 0 and 100% indicating how well the sample spectrum matches the reference spectrum. A value of 100% indicates the spectra and/or profiles are identical.[20−23] The development and application of this quantitative comparison of the similarity of different spectra have been described in detail in previous publications.[22,23] The qualification involved comparing the spectral similarity obtained by computer mixing of the spectra of the protein with different structure versus the spectral similarity obtained upon the actual mixing of combinations of the same proteins with different structures, as well as the analysis of protein spectra in 6 M Gdn. The smaller the spectral similarity number, the more the sample differs from the physical structure of the reference or folded material. Spectral similarity determination provides an objective way to compare any two spectra and can be correlated to the extent of unfolding but is not a direct assessment of unfolding percentage.

Near- and far-UV CD spectra were recorded at ambient temperature on a Jasco J-710 spectropolarimeter. The proteins were analyzed at a concentration of ∼0.5 mg/mL, using cuvettes with a path length of 1 cm for the near-UV CD spectra (240−340 nm) and 0.02 cm for the far-UV CD spectra (195−250 nm). The spectra shown are the average of 12−15 scans with a 0.5 nm step size and a 4 s response time. The CD spectral similarities were obtained with seven-point smoothing of the spectra and 4 nm resolution using the Thermo Electron OMNIC software QC compare function.

The fluorescence spectra were measured with a Hitachi F-4500 fluorescence spectrophotometer using a 0.5 cm path length sample cell. The excitation wavelength was 280 nm for the intrinsic fluorescence spectra. The proteins were diluted to 0.2 mg/mL with the appropriate buffer prior to analysis.

ANS binding was measured with a Hitachi F-4500 fluorescence spectrophotometer using a 0.5 cm path length sample cell. The emission spectrum of ANS was monitored from 400 to 500 nm with ANS concentrations of 50, 75, 100, and 150 μM at different pH values with an excitation wavelength of 380 nm using a 5.0 nm bandwidth. The spectral data shown are single measurements of the average of five scans.

FTIR spectra of protein solutions were recorded at room temperature with a Nicolet Magna 550 series II Fourier transform infrared spectrometer, equipped with a dTGS detector. Protein solutions prepared at 10 mg/mL by concentrating the sample solutions in Millipore Biomax-0.5 filters with a 5000 Da molecular mass cutoff were measured in a sample cell (Spectra-Tech FT04-036) that employed CaF_2 windows separated by a 6 μm Mylar spacer. For each spectrum, a 256-scan interferogram was collected in a single beam mode, with a 4 cm^{-1} resolution. Buffer blank spectra were recorded under identical conditions. The blank spectra and gaseous water were subtracted from the protein spectra, according to previously established criteria. The second-derivative spectrum

was calculated with Thermo Electron OMNIC software. The final spectrum was smoothed with a nine-point function to remove white noise. The FTIR analyses in the amide I region (1600−1700 cm^{-1}) were used for secondary structure comparison, and the spectral similarities were obtained with a 15-point smoothing of the spectra and 8 cm^{-1} resolution using the Thermo Electron OMNIC software QC compare function.

FT-Raman spectra were acquired on a Nicolet FT-Raman 960 spectrometer at ambient temperature in the range of 400−1800 cm^{-1}. The protein solution was concentrated to >50 mg/mL and sealed in quartz capillaries. The spectra were corrected for the contribution from buffer and baseline. The laser power at the sample was maintained at approximately 650−750 mW, and the spectral resolution was 8 cm^{-1}. For secondary structure, amide I (1600−1700 cm^{-1}) and amide III (1200−1350 cm^{-1}) were monitored. For tertiary structure, the following spectral signals were monitored: the Fermi doublet at ∼856 and ∼830 cm^{-1} was monitored for tyrosine hydrogen bonding; the signal at ∼1550 cm^{-1}, which is correlated to the torsion angle of the Cβ−C3 bond, was monitored for the tryptophan indole environment; the signals at ∼1360 and ∼1340 cm^{-1} were monitored for the hydrogen bonding state of the tryptophan indole ring; and the signal between 500 and 560 cm^{-1} of the disulfide stretching mode was used as a sensitive indicator of the disulfide bridge configuration.[24]

The DSC experiments were conducted on a MicroCal VP-DSC in which temperature differences between the reference and sample cell were continuously measured and calibrated to power units. This data channel is termed the DP signal, or the differential power between the reference (buffer) and sample cell. Baseline subtraction was performed by measuring buffer versus buffer and then further analyzed by ORIGIN 7. The samples were heated from 4 to 110 °C at a heating rate of 60 °C/h. The prescan was 15 min, and the filtering period was 10 s. The concentration used in the DSC experiments was ∼0.5 mg/mL.

DLS experiments were performed on the Dynopro-99 (Wyatt, Santa Barbara, CA) using a 830 nm laser as the light source. The samples were prepared in the buffer at 1 mg/mL, by direct dilution of the stock samples in C*x*N buffer for each pH. The solution samples were filtered with a 0.1 μm filter to remove potential dust particles or air bubbles before measurement, and ∼12 μL was used. All DLS measurements were performed at 20 °C. Data were analyzed using the regularization algorithm to obtain the hydrodynamic radius and polydispersity.

Cation exchange chromatography was conducted on an Agilent 1100 HPLC system using a ProPac WCX-10 analytical column preceded by a ProPac WCX-10G guard column, at 25 °C, with 50 μg injection, and a flow rate of 0.7 mL/min. Absorbance was measured at 215 nm. The column was equilibrated with 20 mM sodium acetate (pH 5.2), and protein was eluted with a linear gradient of 20 mM sodium acetate and 300 mM sodium chloride (pH 5.2) from 0 to 100% over 35 min.

Field flow fractionation (FFF) was performed using an Agilent autosampler and pump connected to a Wyatt Eclipse 3 Separation System, with an Agilent UV detector, with the wavelength set to 215 nm, and a Wyatt HELEOS multiangle light scattering (MALS) detector. The separations were performed using a 10 kDa molecular mass cutoff regenerated cellulose membrane in the 25 cm channel with a 490 μm spacer thickness and a 21.5 mm breadth. The tests were conducted at ambient temperature using the corresponding C*x*N buffer for each sample as the respective mobile phase. Neat sample injections of 10 μg of each sample were made onto the FFF system. A focus flow of 2.0 mL/min was applied to the injected sample for 2 min. A channel flow of 1.0 mL/min and a constant crossflow of 2.5 mL/min for 30 min were used for separation.

RESULTS AND DISCUSSION

The Native Higher-Order Structure of IgG1 Fc. The *E. coli*-derived Fc molecule was oxidized and refolded from inclusion bodies, while the CHO-derived Fc molecule was expressed and isolated as the folded, oxidized molecule. Thus, there is the potential for the protein derived from *E. coli* to be slightly misfolded compared to the protein derived from CHO. To ensure that the *E. coli*-derived Fc molecule is folded properly with similar higher-order structure, including disulfide configuration, several techniques were used to assess the structure of the proteins at neutral pH before any stability studies were conducted. Reduced and nonreduced SDS−PAGE were used to confirm the purity of Fc from both sources. Nonreduced peptide maps were used to confirm the disulfide configuration of Fc from both sources. The nonreduced peptide maps of both *E. coli*- and CHO-derived Fc molecules are similar, with the difference in the peaks related to the presence of the carbohydrate in the C_H2 domain of CHO Fc. This indicates that the disulfide configurations of the *E. coli* and CHO-derived Fc molecules are identical. FT-Raman spectroscopy can be used to monitor both the secondary and tertiary structure of protein; the spectra of both the *E. coli*- and CHO-derived Fc molecules are shown in Figure 1 for this comparison. At neutral pH, the Raman spectra of both those Fc molecules have an amide I peak at ∼1670 cm^{-1}, an amide III peak at ∼1240 cm^{-1}, and an amide IV peak at ∼960 cm^{-1}. These peak positions indicate that β-sheet is the primary secondary structure of both the *E. coli*- and CHO-derived Fc molecules. The 850 cm^{-1}/830 cm^{-1} intensity ratio that is sensitive to Tyr hydrogen bonding states is identical for both Fc molecules, suggesting that the average Tyr environments of both molecules are similar. The 1360 cm^{-1}/1340 cm^{-1} intensity ratio that is sensitive to the Trp side chain environment is also similar in both molecules, suggesting that the average Trp environments of both molecules are very similar. Similar results were also obtained by FTIR and far-UV CD. All data suggest that the *E. coli*-derived refolded Fc molecule is properly folded and has secondary and tertiary structure very similar and a disulfide configuration identical to that of the CHO-derived Fc molecule. Any differences that we observed in the stability

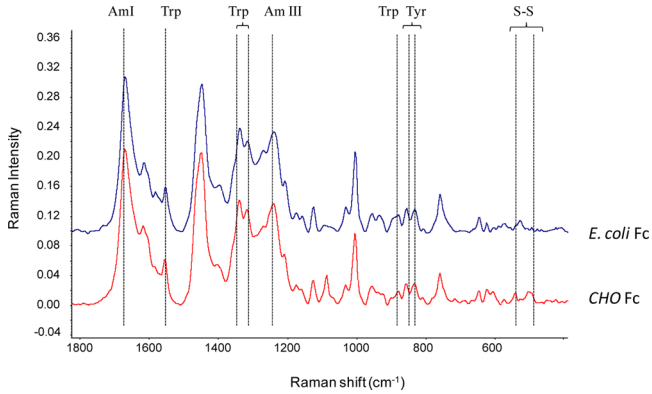

Figure 1. FT-Raman spectra of *E. coli*- and CHO-derived Fc molecules at pH 7.

dx.doi.org/10.1021/bi300702e | *Biochemistry* 2012, 51, 10056−10065

studies are therefore due to differences in the carbohydrate content.

pH-Dependent Conformational Stability. During downstream processing of protein products, low-pH buffers are commonly used to elute protein from columns, and for viral inactivation. It is important to understand the pH stability of the protein solution under conditions that may occur during downstream processing. The stability of both *E. coli*- and CHO-derived Fc molecules to acid-induced changes was assessed by several biophysical techniques. The tertiary structure was assessed by near-UV CD and fluorescence spectroscopies. The spectral similarity of the near-UV CD spectra of the two molecules from pH 2 to 10 compared to the reference pH 7 spectra is plotted in Figure 2A, and representative CD spectra

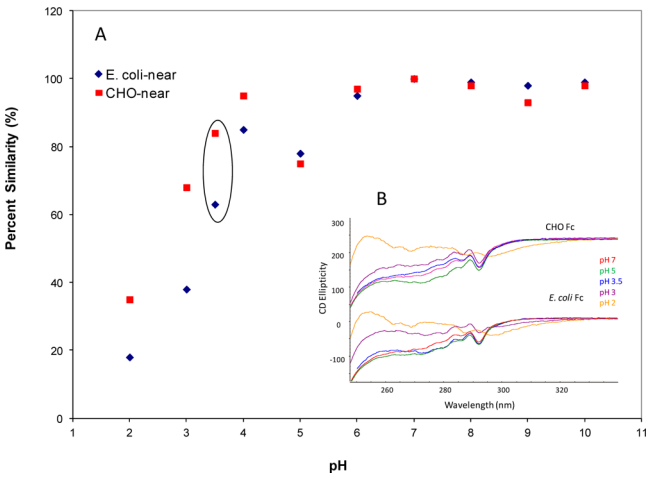

Figure 2. (A) Near-UV CD spectral similarity of *E. coli*- and CHO-derived Fc molecules at different pH values and (B) representative near-UV CD spectra of *E. coli*- and CHO-derived Fc molecules at different pH values.

are shown in Figure 2B. At neutral pH, the spectra of both *E. coli*- and CHO-derived Fc are equivalent. The near-UV CD spectra of Fc from both sources all have minima at 294 nm that can be attributed to tryptophan, features at 289 and 284 nm that can be attributed to tyrosine and tryptophan, features at 274 nm that can be attributed to tyrosine, and fine structure from 250 to 265 nm that can be attributed to the phenylalanines.[25] Significant changes in near-UV CD spectra are seen at pH 3.5 and below for the *E. coli*-derived Fc molecule and at pH 3 and below for the CHO-derived material, with a decrease in the level of spectral similarity (Figure 2). The spectral similarity correlates the overall spectral information in the specified region of the sample and the reference spectra to determine the similarity between the sample spectrum and the reference spectrum, with 100% indicating identity. This method has been described in detail in previous publications.[22,23] For these methods, values of ≥90% indicate that there is no significant difference between the samples (i.e., the value is within the usually experimental variability). The lower the spectral similarity, the larger the difference in spectra, and therefore, there is a difference in protein structure between the two proteins. At pH 3.5, there is a greater loss of tertiary structure for the *E. coli*-derived Fc molecule than the CHO-derived Fc molecule, demonstrated by the lower level of spectral similarity obtained for *E. coli*-derived Fc. This indicates that the CHO-derived Fc molecule retains more native structure and is more stable to pH-induced unfolding. At pH 2, the unfolded structure of the two proteins appears to be very similar if not identical, with a significant decrease in the level of spectral similarity compared to its pH 7 spectra. At pH 5, there is a dip in the level of spectral similarity for both *E. coli*- and CHO-derived Fc molecules. The decrease in the level of spectral similarity at pH 5 is due to the spectral differences in the 260−280 nm region that are attributed to the disulfide signal. The intensity of this region reflects the disulfide bond environment of the Fc protein. The data indicate that the disulfide environment at pH 5 is altered compared to that at pH 7 for both *E. coli*- and CHO-derived Fc in a manner independent of the presence of carbohydrate. Similar results were also observed from the fluorescence analysis of both Fc molecules at different pH values, and changes in the protein conformation can be seen at low pH. ANS binding was used as a probe for unfolding-induced perturbations in the surface of the two proteins. The ANS fluorescence intensities at 480 nm as a function of pH are plotted in Figure 3. From pH 10 to 5,

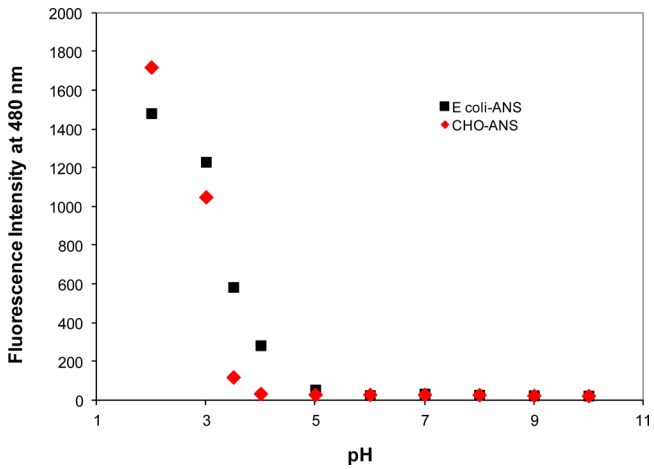

Figure 3. ANS binding of *E. coli*- and CHO-derived Fc molecules at 480 nm with 50 μM ANS as a function of pH.

ANS fluorescence at 480 nm, 50 μM for both *E. coli*- and *CHO*-derived Fc, is similar, with very low intensity. This indicates that both proteins remain folded in the native conformation, with a very hydrophilic surface under these solution conditions, as seen previously.[26,27] As the pH decreases from 5 to 2, the ANS fluorescence intensity starts to increase significantly at pH ≤4 for the *E. coli*-derived Fc molecule and at pH ≤3.5 for the CHO-derived Fc molecule, indicating that unfolding begins to occur under these low-pH conditions and that the CHO-derived molecule is slightly more stable to acid-induced unfolding than the *E. coli*-derived molecule, consistent with the near-UV CD results.

The secondary structure of both Fc molecules as a function of pH was analyzed by FTIR and far-UV CD spectroscopy. The FTIR spectral similarity of both *E. coli*- and CHO-derived Fc molecules at different pH values compared to the FTIR spectra of the corresponding protein at pH 7 are plotted in Figure 4A, and representative second-derivative FTIR spectra of *E. coli*-derived Fc at different pH values are shown in Figure 4B. The spectra of both the *E. coli*- and CHO-derived protein at pH 7 have a level of spectral similarity of >91%, indicating that Fc molecules from both sources have similar secondary structures. From pH 4 to 10, the FTIR spectra of both Fc molecules are

dx.doi.org/10.1021/bi300702e | *Biochemistry* 2012, 51, 10056−10065

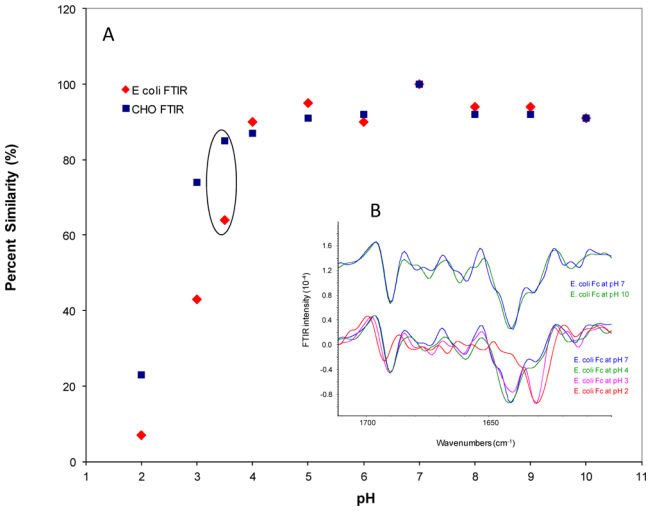

Figure 4. (A) FTIR spectral similarity of *E. coli*- and CHO-derived Fc molecules at different pH values and (B) representative FTIR spectra of the *E. coli*-derived Fc molecule at different pH values.

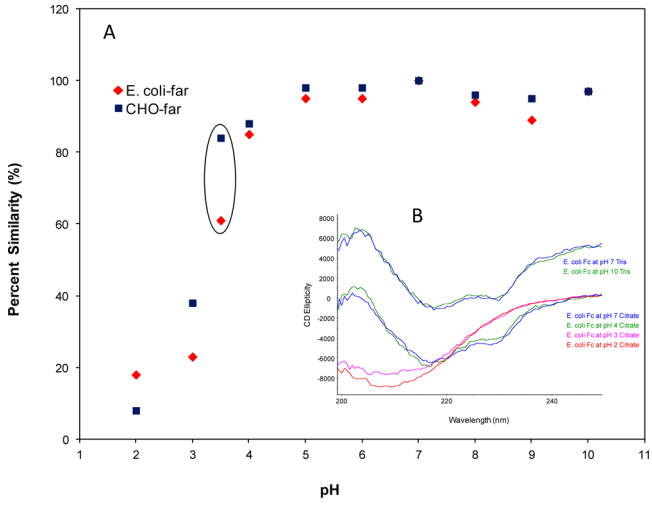

Figure 5. (A) Far-UV CD spectral similarity of *E. coli*- and CHO-derived molecules at different pH values and (B) representative far-UV CD spectra of the *E. coli*-derived Fc molecules at different pH values.

similar and show strong β-sheet bands at 1642, 1631, and 1690 cm^{-1}, indicating the presence of predominantly antiparallel β-sheet secondary structure[28−30] with a level of spectral similarity compared to the spectrum at neutral pH of >90%, suggesting that the folded secondary structure is maintained under these conditions[20−23] for both molecules. At pH 3, the CHO-derived Fc spectrum shows an increase in the intensity of the intermolecular β-sheet band at 1631 cm^{-1} and a shift of the 1690 cm^{-1} band to 1693 cm^{-1} with an accompanying significant decrease in the level of spectral similarity to 74%; this occurs for the *E. coli*-derived molecule at pH 3.5. These results indicate the formation of intermolecular β-sheet secondary structure[30] at pH ≤3 for both Fc molecules, with the secondary structure of the glycosylated Fc molecule being more stable to low-pH-induced unfolding than that of the aglycosylated Fc. Similar results were obtained from far-UV CD spectroscopic analysis. The far-UV CD spectral similarity of both *E. coli*- and CHO-derived Fc molecules at different pH values compared to the far-UV CD spectra at pH 7 is plotted in Figure 5A, and representative far-UV CD spectra of the *E. coli*-derived Fc molecule are shown in Figure 5B. The slight difference in the far-UV CD spectra at pH 7 in the different buffers may be due to the buffer interference in this region for which buffer subtraction cannot fully account. The far-UV CD spectra of both Fc molecules at pH 7 have a level of spectral similarity of >96%, again confirming that the Fc molecules from both sources have similar secondary structure. From pH 4 to 10, all spectra remain unchanged with minima at 230 and 217 nm, indicating that the proteins contain primarily β-sheet and β-turn structures. The minima at 230 nm in these spectra are also seen in the spectra of IgG1 antibodies and contain contributions from ring stacking[8,31,32] as well as β-sheet secondary structure. The secondary structure of the *E. coli*-derived Fc molecule begins to unfold at pH 3.5, while the CHO-derived Fc molecule still retains most of its native secondary structure under these conditions. At pH ≤3, both proteins have lost secondary structure, with a shift in the minimum from 217 to 200 nm, the minimum at 230 nm no longer apparent, and a decrease in the level of spectral similarity when compared to their corresponding pH 7 spectra. At pH 2, the spectra of both proteins are quite different from that of the native proteins with a level of spectral similarity of <20% versus the pH 7 spectra of the corresponding proteins. This indicates a substantial loss of native secondary structure.

pH-Dependent Thermal Stability. A previous study by Wen et al showed that protein stability is correlated with thermal stability. In their study, the authors show that the protein with the higher thermal melting temperature exhibits better long-term stability.[33] Assessing the pH-dependent thermal stability helps us to understand and predict the long-term stability of the Fc molecule, and DSC was used to analyze the thermal stability of a protein (or a protein domain) under different solvent conditions. The DSC profiles of *E. coli*- and CHO-derived Fc at pH 7 in citrate and Tris buffers are shown in Figure 6. The first peak (T_{m1}) is from the unfolding of the

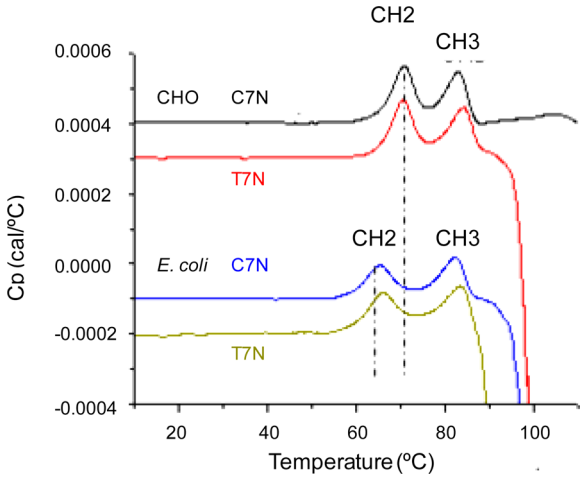

Figure 6. DSC profiles of *E. coli*- and CHO-derived Fc molecules in Tris (T7N) and citrate (C7N) buffers at pH 7.

C_H2 domain, and the second peak (T_{m2}) is from the unfolding of the C_H3 domain.[33−37] The exotherm following the transition of the C_H3 domain is believed to be the result of precipitation of the heat-induced unfolded protein, and particulates were observed after the heat unfolding of both Fc molecules. The T_{m1} of CHO-derived Fc is ∼5 °C higher than the T_{m1} of *E. coli*-derived Fc at neutral pH; the C_H3 domain transitions (T_{m2}) are

dx.doi.org/10.1021/bi300702e | *Biochemistry* 2012, 51, 10056−10065

very similar, and the heat-induced unfolded forms of CHO-derived Fc remain in solution under conditions where the unfolded forms of *E. coli*-derived Fc aggregate. This is especially true in citrate buffer (C7N) where the exotherm was seen for the *E. coli*-derived Fc but not for the CHO-derived Fc protein (Figure 6). This observation suggests that the glycosylation of the C_H2 domain of Fc stabilizes this part of the Fc molecule and results in a higher C_H2 domain thermal transition compared to that of the aglycosylated *E. coli*-derived Fc molecule. The glycosylation also appears to increase the solubility of the heat-induced unfolded Fc molecule. The plots of T_{m1} and T_{m2} of *E. coli*- and CHO-derived Fc versus pH are shown in Figure 7A. Both *E. coli*- and CHO-derived Fc

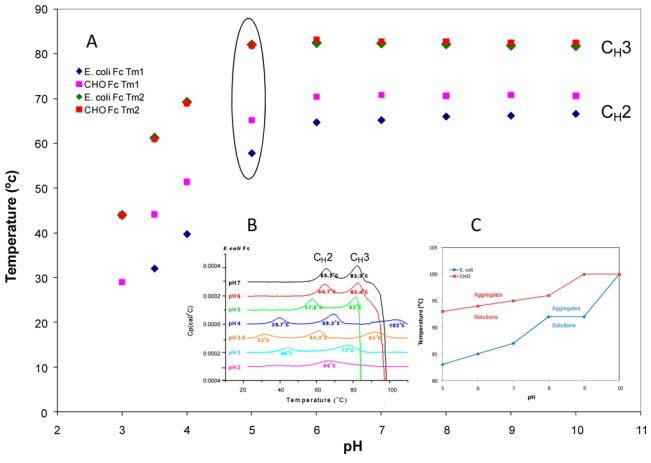

Figure 7. (A) C_H2 (T_{m1}) and C_H3 (T_{m2}) domain melting of *E. coli*- and CHO-derived Fc molecules from pH 2 to 10. (B) Representative DSC profiles of the *E. coli*-derived Fc molecule from pH 2 to 7. (C) Solubility diagram of *E. coli*- and CHO-derived Fc molecules at different pH values and temperatures.

molecules had two major endothermic peaks, T_{m1} and T_{m2}, before the protein precipitated out of the solution. The *E. coli*-derived molecule has a lower C_H2 (T_{m1}) domain melting transition compared to CHO-derived Fc, while the T_{m2} values of both Fc molecules are identical from pH 5 to 10. Representative DSC scans of *E. coli*-derived Fc from pH 2 to 7 in 20 mM citrate with 140 mM NaCl are shown in Figure 7B, and the exotherm temperatures from pH 5 to 10 are plotted in Figure 7C to better visualize the heat-induced unfolding and aggregation phenomena. At pH 5, the C_H2 domain melting transition (T_{m1}) decreases from ~65 to ~58 °C while the C_H3 domain melting transition (T_{m2}) remains relatively unchanged (~82 °C) for the *E. coli*-derived Fc molecule. Similar results are also observed for the CHO-derived Fc molecule at a lower pH (pH 4). This observation suggests that the heat-induced unfolding of both Fc molecules involves at least two steps: the C_H2 domain unfolding first followed by the C_H3 domain unfolding. The aggregation of the heat-induced unfolded form was the most significant at pH 5 as seen by the exotherm at 83 °C for the *E. coli*-derived Fc and 93 °C for the CHO-derived Fc following the C_H3 domain transition (Figure 7B,C) under identical solution conditions. At pH 4 and 3.5, the C_H2 and C_H3 domain transition temperatures decreased for both Fc molecules (Figure 7A,B), and the unfolded form did not precipitate out off solution; instead, a third endothermic peak was observed at a higher temperature. The endothermic transition at a high temperature in acidic solutions has been discussed previously for IgG mAbs; its assignment remains unclear.[14] It most likely is the combination of the changes in conformation and the aggregation state. At pH 3, the C_H2 domain melting transition (T_{m1}) has completely disappeared and only the C_H3 domain melting transition (T_{m2}) is observed for the *E. coli*-derived Fc molecule, while the C_H2 domain melting transition (T_{m1}) and the C_H3 domain melting transition (T_{m2}) are still observed for the CHO-derived Fc. This further confirmed that the CHO-derived Fc is more stable to heat-induced unfolding than the *E. coli*-derived molecule under the same solution conditions. At pH 2, both Fc molecules are unfolded by acid, and neither the C_H2 nor the C_H3 domain melting transition is observed.

pH-Dependent Size Distribution and Heterogeneity. The hydrodynamic properties and size distribution of the proteins as a function of pH are also important parameters that may affect downstream processing and long-term stability. The hydrodynamic properties of the proteins in citrate at neutral pH and physiological salt concentration were assessed by DLS. The *E. coli*-derived Fc molecule has an R_h of 4.3 nm and a polydispersity of 26%, while the CHO-derived molecule has an R_h of 3.7 nm and a polydispersity of 21%. At neutral pH, the CHO-derived Fc (glycosylated protein) has a smaller hydrodynamic radius than the *E. coli*-derived Fc (aglycosylated protein), in spite of the presence of the two carbohydrates on this protein. Unlike the majority of glycoproteins, for example, EPO, where the large carbohydrate chain moieties are on the protein surface,[38] the two carbohydrates of Fc are located in the interior of the C_H2 domains of the Fc dimer. These data suggest that they are interacting with each other and/or amino acid residues in this region, resulting in a more compact structure of the Fc molecule. This observation is consistent with the X-ray diffraction results that show the intercarbohydrate chain of the human Fc molecule contacts between the two C_H2 domains and exists as a "weak ridge"[39,40] and also consistent with the increased sensitivity to proteases seen with the protein upon the removal of the sugars.[4] It is also consistent with the findings presented here that the glycosylated Fc molecule is more stable to thermally induced and low-pH-induced unfolding than the aglycosylated Fc molecule, even though they have the same folded solution structure at neutral pH.

The size distribution and heterogeneity of the Fc solutions at different pH values were analyzed by FFF and cation exchange chromatography.[41] FFF was run in the appropriate sample buffer. CEX was selected as the percentage of high-molecular weight species (HMWS), insoluble aggregates, and other chemical modifications can be quantified on the basis of the loss of monomer using this technique. Results from both FFF and cation exchange chromatography show that some high-molecular weight species are present at low pH. At pH ≤3.0, the *E. coli*-derived Fc molecule has little monomer remaining while the CHO-derived Fc molecule is still primarily monomeric, as seen by the CEX analysis (Figure 8).

Effect of Salt on Conformation and Thermal Stability. Salt is often used during downstream processing of protein and sometimes is also used as an excipient of the formulation matrix. Protein denaturation is often dependent on the exact buffer composition and the salt concentration in which the reaction is occurring. Indeed, the DSC results described above demonstrate that the Fc protein thermally unfolds differently in citrate versus Tris buffers. To understand this further, the effect of NaCl concentration on the unfolding of both *E. coli*- and

dx.doi.org/10.1021/bi300702e | *Biochemistry* 2012, 51, 10056−10065

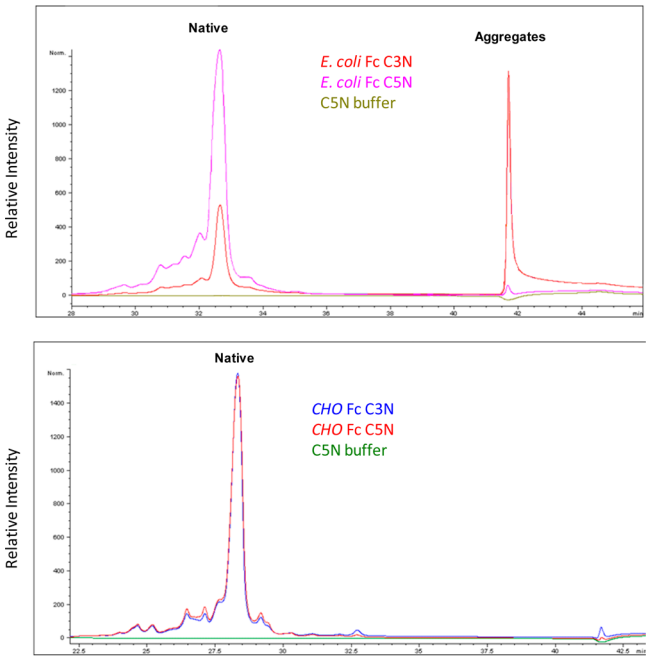

Figure 8. Representative CEX chromatogram of the *E. coli*- and CHO-derived Fc molecules at different pH values.

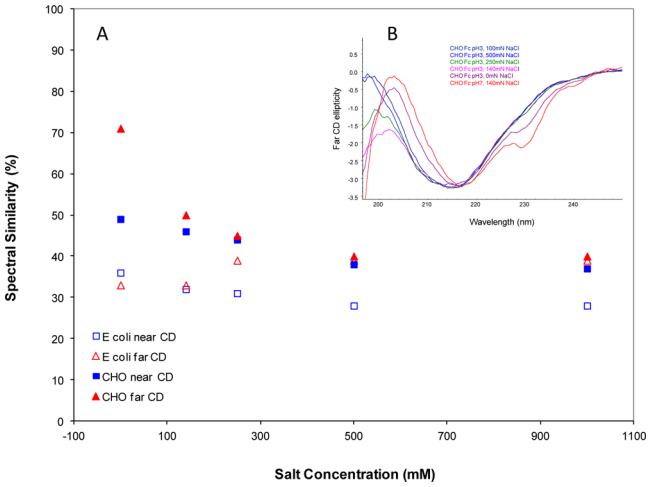

Figure 9. (A) Near- and far-UV CD spectral similarity of *E. coli*- and CHO-derived Fc molecules and (B) selected far-UV CD of the CHO-derived Fc at pH 3 as a function of salt concentration.

CHO-derived Fc was studied. The secondary structures and hydrodynamic radii of both proteins at pH 7 do not appear to be affected by salt concentration when analyzed by far-UV CD and FTIR and dynamic light scattering. This indicates that the native secondary structure of the Fc molecule at pH 7 is maintained in the presence of 0−1000 mM NaCl at ambient temperature regardless of the absence or presence of glycosylation. The changes in the ionic strength with an increasing salt concentration have little effect on the structure and self-association of both molecules, suggesting that the electrostatic charge interactions between the proteins do not significantly impact the structure of the folded Fc molecules.

At pH 3, the results obtained by increasing the salt concentration to change the ionic strength of the solution are more complicated. The *E. coli*-derived Fc molecule at pH 3 has very little tertiary structure in the presence of 0 mM NaCl. Increasing the ionic strength by increasing the salt concentration has little effect on the secondary and tertiary structure of the unfolded intermediate, monitored by near- and far-UV CD. In contrast, the CHO-derived Fc molecule at pH 3 without salt is partially unfolded, with some native structure remaining; this partially unfolded state is further unfolded with an increase in salt concentration until it becomes equivalent to the *E. coli*-derived Fc intermediate at pH 3. The levels of spectral similarity of the near- and far-UV CD spectra of both proteins at pH 3 compared to the spectra in C7N as a function of salt concentration are shown in Figure 9A. Representative far-UV CD spectra of the CHO-derived Fc as a function of salt concentration are shown in Figure 9B. As the salt concentration is increased, there is a simultaneous increase in the level of intermolecular β-sheet as seen by the intensity change at 200 nm and a decrease in the intensity of the 230 nm shoulder. Similar results were also obtained by FTIR analysis. Both UV CD and FTIR results indicate that the CHO-derived protein is partially unfolded and has a considerable amount of native secondary and tertiary structure present at pH 3 with 0 M NaCl. Increasing the salt concentration from 0 to 140 mM in the solution will mask the surface charge, decrease the extent of electrostatic charge repulsion between protein molecules, and favor hydrophobic interactions, resulting in the further unfolding and self-association of the partially unfolded CHO-derived molecule. This unfolded form of the CHO-derived Fc molecule once obtained at pH 3 with 140 mM NaCl appears to be similar to the unfolded form of the aglycosylated protein at pH 3 at all ionic strengths tested and is not affected further by continued increases in salt concentration. These results are also consistent with recent reports that there are specific interactions between salts and charged residues on the surface of the protein, and increasing salt concentrations can mask these surface charges and result in decreased protein stability.[42−49]

The thermal stabilities of both *E. coli*- and CHO-derived Fc were also compared as a function of salt concentration at pH 7, 5, and 3 by DSC. At pH 7 and 5, both T_{m1} and T_{m2} were observed as the salt concentration increased from 0 to 500 mM NaCl and the T_{m1} corresponding to the C_H2 domain unfolding decreases slightly (3−5 °C) with an increasing salt conentration. At pH 3, the C_H3 domain melting transition (T_{m2}) is the only transition observed for the *E. coli*-derived Fc molecule, while both transitions T_{m1} and T_{m2} can be seen for the CHO-derived Fc molecule. Figure 10 shows the different unfolding states as defined by the domain conformations at pH 3, as a function of salt concentration and temperature. There are three states that can be seen depending on the solution conditions. State 1 is defined as that in which both C_H2 and C_H3 domain thermal transitions are present; state 2 is defined as that in which only the thermal transition from the C_H3 domain is present, and state 3 is defined as that in which no C_H2 nor C_H3 domain thermal transitions are seen. Under the same solution conditions, all three states (1−3) are observed for CHO-derived Fc at pH 3, while there is no state 1 for the *E. coli*-derived aglycosylated protein. As the salt concentration is increased from 0 to 140 mM at pH 3, T_{m2} decreases for both Fc molecules (Figure 10A,B) and T_{m1}, which is only present for the CHO-derived protein, decreases as well. These data demonstrate that increasing the salt concentration from 0 to 500 mM decreases the stability of the C_H2 and C_H3 domains. At pH 3 with 1000 mM salt, neither T_{m1} nor T_{m2} is observed for the *E. coli*-derived molecule while both T_{m1} and T_{m2} are still

dx.doi.org/10.1021/bi300702e | *Biochemistry* 2012, 51, 10056−10065

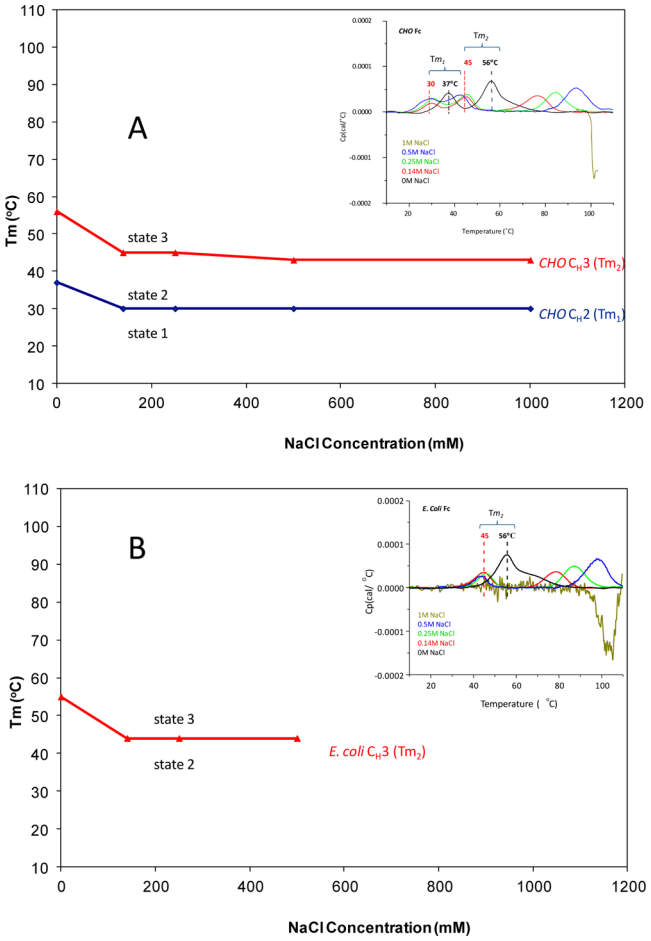

Figure 10. (A) C_H2 (T_{m1}) and C_H3 (T_{m2}) domain melting of CHO-derived Fc and representative DSC profiles of CHO-derived Fc at pH 3 as a function of salt concentration. (B) C_H3 (T_{m2}) domain melting of *E. coli*-derived Fc and representative DSC profiles of *E. coli*-derived Fc at pH 3 as a function of salt concentration.

present for CHO-derived Fc (Figure 10A,B). This again demonstrates that the CHO-derived Fc molecule is more stable and retains more structure than the *E. coli*-derived Fc molecule under extreme solution conditions and is consistent with the pH stability result described previously.

Reversibility of Low-pH-Induced Conformational Changes. During downstream processing of protein products, after the protein is exposed to low-pH buffers (e.g., protein A column elution and viral inactivation) for a short period of time, the protein solution is quickly neutralized to pH 5 or 7 and remains at this pH for processing and delivery. Therefore, it is important to understand the reversibility of low-pH-induced conformational changes after the protein solution is neutralized to pH 7. Previous studies of both antibodies and other proteins have demonstrated that the formation of the intermolecular β-sheet is irreversible, often resulting in aggregation and precipitation.[14] To see if less dramatic pH-induced changes in conformation were reversible, we analyzed the reversibility of conformational changes induced by exposure of both *E. coli*- and CHO-derived Fc molecules to pH 3 and 3.5 with the pH 7 samples as a control. The DSC profiles, second-derivative FTIR and far-UV CD spectra of both *E. coli*- and CHO-derived Fc molecules in PBS following incubation in the pH 3, 3.5, and 7 citrate buffers for 2 h at room temperature are very similar, indicating that the thermally induced global unfolding of the protein domains and the secondary structural changes induced at pH 3 and 3.5 are reversible. There are only very subtle irreversible changes in the disulfide conformations and surface hydrophobicity of the protein as observed by near-UV CD and ANS binding for the *E. coli*-derived Fc molecule but not for the CHO-derived Fc molecule. The 50 μM ANS fluorescence intensities, an indicator of perturbations in protein surface, are shown in Figure 11. The data show that the *E. coli*-

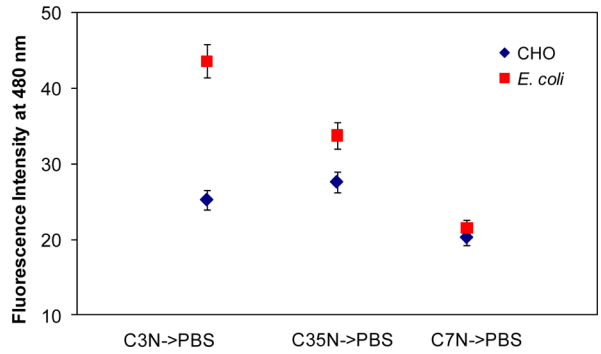

Figure 11. ANS binding at 50 μM for *E. coil*- and CHO-derived Fc molecules in PBS after incubation at pH 3, 3.5, and 7 at room temperature for 2 h.

derived Fc molecule in PBS after incubation at pH 3 shows significantly stronger ANS binding compared to the protein incubated in pH 7, while the CHO-derived Fc has similar ANS binding, demonstrating that even though there are no irreversible changes detected in the heat-induced global unfolding of the protein domains and the secondary structure at pH 3, the exposure of *E. coli*-derived Fc to pH 3 leads to irreversible changes in the disulfide environment and surface hydrophobicity of the molecule. In contrast, the surface changes that occurred with CHO-derived Fc at pH 3 appear to be reversible.

CONCLUSION

This study probed the effect of pH, temperature, and salt on the stability of *E. coli*- and CHO-derived IgG1 Fc and glycosylation on the solution structure and stability of IgG1 Fc. These results, taken together, demonstrate that the IgG1 Fc molecule unfolds in a multistep reaction when stressed by heat and/or pH that can result in the formation of partially unfolded intermediates and aggregates that are stable enough to be characterized. The exact state of the Fc molecule depends on pH, ionic strength, buffer composition, and temperature. Glycosylation of Fc results in a slightly more compact, stable molecule and decreases the level of self-association of the partially unfolded intermediate forms without changing the native conformation of IgG1 Fc. For optimal production yield and long-term storage stability, these conditions need to be carefully managed. Further studies of the interaction of salt with the IgG1 Fc molecules are necessary to improve our understanding of the complicated interactions of buffer components with the various domains and intermediates of IgG1 Fc that have been demonstrated to exist as a function of pH, buffer composition, and temperature.

dx.doi.org/10.1021/bi300702e | *Biochemistry* 2012, 51, 10056−10065

■ ASSOCIATED CONTENT

Supporting Information

Reduced and nonreduced SDS−PAGE for both *E. coil*- and CHO-derived Fc molecules showing that the preparations of both *E. coil*- and CHO-derived Fc molecules are >95% pure. This material is available free of charge via the Internet at http://pubs.acs.org.

■ AUTHOR INFORMATION

Corresponding Author

*Product Attribute Sciences, Amgen Inc., Thousand Oaks, CA 91320. C.H.L.: telephone, (805) 447-1151; e-mail, cynthial@amgen.com. Y.J.: telephone, (805) 447-1116; e-mail, yjiang@amgen.com.

Funding

This work is funded by Amgen Inc.

Notes

The authors declare no competing financial interest.

■ ACKNOWLEDGMENTS

We thank Tom Boone, Mike Mann, Lisa Rensshaw-Gegg, Helen Kim, Shirley Stevenson, Robert Rosenfeld, and Ling Cai for cloning, expression, and purification of the IgG Fc used in these studies, Quanzhou Luo for nonreduced peptide map analysis of IgG Fc to confirm the disulfide configuration, and Frank Martin, David Brems, and Rohini Deshpande for helpful discussions of the results.

■ ABBREVIATIONS

CD, circular dichroism; FTIR, Fourier transform infrared; FT-Raman, Fourier transform Raman; ANS, 1,8-(anilino)-naphthalene sulfonate; CHO, Chinese hamster ovary cells; DDT, dichlorodiphenyltrichloroethane; SDS−PAGE, sodium dodecyl sulfate−polyacrylamide gel electrophoresis; DLS, dynamic light scattering; DSC, differential scanning calorimetry; PBS, phosphate-buffered saline; C*x*N, citrate buffer with sodium chloride at pH *x*; T*x*N, Tris buffer at pH *x* with NaCl; CEX, cation exchange chromatography; FFF, field flow fractionation; mAb, monoclonal antibody; HMWS, high-molecular weight species.

■ REFERENCES

(1) Hui, H., Farilla, L., Merkel, P., and Perfetti, R. (2002) The short half-life of glucagon-like peptide-1 in plasma does not reflect its long-lasting beneficial effects. *Eur. J. Endocrinol. 146*, 863−869.

(2) Oshima, I., Hirota, M., Ohboshi, C., and Shima, K. (1998) Comparison of half disappearance times, distribution volumes and metabolic clearance rates of exogenous glucagon-like peptide 1 and glucagon in rats. *Regul. Pept. 21*, 85−93.

(3) Huang, C. (2009) Receptor-Fc fusion therapeutics, traps, and MIMETIBODY technology. *Curr. Opin. Biotechnol. 20*, 692−699.

(4) Tao, M.-H., and Morrison, S. L. (1989) Studies of Aglycosylated Chimeric Mouse-Human IgG: Role of Carbohydrate in the Structure and Effector Functions Mediated by the Human IgG Constant Region. *J. Immunol. 143*, 2595−2601.

(5) Wright, A., and Morrison, S. L. (1997) Effect of glycosylation on antibody function: Implications for genetic engineering. *Trends Biotechnol. 15*, 26−32.

(6) Goto, Y., and Hamaguchi, Y. (1982) Unfolding and refolding of the reduced constant fragment of the immunoglobulin light chain: Kinetic role of the intrachain disulfide bond. *J. Mol. Biol. 156*, 911−926.

(7) Lilie, H., McLaughlin, S., Freedman, R., and Buchner, J. (1994) Influence of Protein Disulfide Isomerase (PDI) on Antibody Folding *in Vitro*. *J. Biol. Chem. 269*, 14290−14296.

(8) Vermeer, A. W. P., and Norde, W. (2000) The thermal stability of immunoglobulin: Unfolding and aggregation of a multi-domain protein. *Biophys. J. 78*, 394−404.

(9) Vermeer, A. W. P., Norde, W., and van Amerongen, A. (2000) The Unfolding/Denaturation of Immunogammaglobulin of Isotype 2b and its F_{ab} and F_c Fragments. *Biophys. J. 79*, 2150−2154.

(10) Vinci, F., Catharino, S., Frey, S., Buchner, J., Marino, G., Pucci, P., and Ruoppolo, M. (2004) Hierarchical Formation of Disulfide Bonds in the Immunoglobulin Fc Fragment Is Assisted by Protein-disulfide Isomerase. *J. Biol. Chem. 279*, 15059−15066.

(11) Feige, M. J., Walter, S., and Buchner, J. (2004) Folding Mechanism of the C_H2 Antibody Domain. *J. Mol. Biol. 344*, 107−118.

(12) Lilie, H., Jaenicke, R., and Buchner, J. (1995) Characterization of a quaternary-structured folding intermediate of an antibody Fab-fragment. *Protein Sci. 4*, 917−924.

(13) Thies, M. J. W., Kammermeier, R., Richter, K., and Buchner, J. (2001) The alternatively folded state of the antibody C_H3 domain. *J. Mol. Biol. 309*, 1077−1085.

(14) Ejima, D., Tsumoto, K., Fukada, H., Yumioka, R., Nagase, K., Arakawa, T., and Philo, J. S. (2007) Effects of Acid Exposure on the Conformation, Stability, and Aggregation of Monoclonal Antibodies. *Proteins: Struct., Funct., Bioinf. 66*, 954−962.

(15) Chaudhuri, A. R., Khan, I. A., and Luduena, R. F. (2001) Detection of disulfide bonds in bovine brain tubulin and their role in protein folding and microtubule assembly in vitro: A novel disulfide detection approach. *Biochemistry 40* (30), 8834−8841.

(16) Wedemeyer, W. J., Welker, E., Narayan, M., and Scheraga, H. A. (2000) Disulfide bonds and protein folding. *Biochemistry 39* (15), 4207−4216.

(17) Mamathambika, B. S., and Bardwell, J. C. (2008) Disulfide-linked protein folding pathways. *Annu. Rev. Cell Dev. Biol. 24*, 211−235.

(18) Tischenko, V. M., Abramov, V. M., and Zav'yalov, V. P. (1998) Investigation of the Cooperative Structure of Fc Fragments from Myeloma Immunoglobulin G. *Biochemistry 37*, 5576−5581.

(19) Martsev, S. P., Kravchuk, Z. I., and Vlasov, A. P. (1994) Large increase in thermal stability of the CH3 domain of rabbit IgG after acid treatment as evidenced by differential scanning calorimetry. *Immunol. Lett. 43*, 149−152.

(20) Ominic software manual.

(21) Cover, T. M., and Hart, P. E. (1967) Nearest Neighbor Pattern Classification. *IEEE Trans. Inf. Theory IT-13* (1), 21−27.

(22) Li, C., Nguyen, X., Narhi, L., Chemmalil, L., Towers, E., Muzammil, S., Gabrielson, J., and Jiang, Y. (2011) Applications of circular dichroism for structural analysis of proteins: Qualification of near- and far-UV CD for protein higher order structural analysis. *J. Pharm. Sci. 100*, 4631−4642.

(23) Jiang, Y., Li, C., Nguyen, X., Muzammil, S., Towers, E., John Gabrielson, J., and Narhi, L. (2011) Qualification of FTIR spectroscopic method for protein secondary structural analysis. *J. Pharm. Sci. 100*, 4642−4654.

(24) Li, H., Hanson, C., Fuchs, J. A., Woodward, C., and Thomas, G. J., Jr. (1993) Determination of the pKa Values of Active-Center Cysteines, Cysteines-32 and -35, in *Escherichia coli* Thioredoxin by Raman Spectroscopy. *Biochemistry 32*, 5800−5808.

(25) Rava, R. P., and Spiro, T. G. (1985) Resonance Enhancement in the Ultraviolet Raman Spectra of Aromatic Amino Acids. *J. Phys. Chem. 89*, 1856−1861.

(26) He, F., Phan, D. H., Hogan, S., Bailey, R., Becker, G. W., Narhi, L. O., and Razinkov, V. I. (2010) Detection of IgG aggregation by a high throughput method based on extrinsic fluorescence. *J. Pharm. Sci. 99* (6), 2598−2608.

(27) Parker, C. W., and Osterland, C. K. (1970) Hydrophobic Binding Sites on Immunoglobulins. *Biochemistry 9*, 1074−1082.

(28) Dong, A., and Caughey, W. S. (1994) Infrared methods for study of hemoglobin reactions and structures. *Methods Enzymol. 232*, 139−175.
(29) Dong, A., Huang, P., and Caughey, W. S. (1990) Protein secondary structures in water from second-derivative amide I infrared spectra. *Biochemistry 29*, 3303−3308.
(30) Li, C. H., and Li, T. (2009) Application of Vibrational Spectroscopy to the Structural Characterization of Human Monoclonal Antibody and its Aggregations During Formulation Development. *Curr. Pharm. Biotechnol. 10*, 391−399.
(31) Woody, R. W. (1994) Contributions of tryptophan side chains to the far-ultravoilet circular dichroism of protein. *Eur. Biophys. J. 23*, 253−262.
(32) Manning, M. C., and Woody, R. W. (1989) Theoretical Study of the Contribution of Aromatic Side Chains to the Circular Dichroism of Basic Bovine Pancreatic Trypsin Inhibitor. *Biochemistry 28*, 8609−8613.
(33) Wen, J., Jiang, Y., and Narhi, L. (2008) Effect of Carbohydrate on Thermal Stability of Antibodies. *Am. Pharm. Rev. 11* (6), 98−104.
(34) Wen, J., Jiang, Y., Hymes, K., Gong, K., and Narhi, L. (2007) Using Differential Scanning Calorimetry in Understanding the Correlation Between Thermal Stability and Protein Stability: A Case Study. MicroCal Application Note, MicroCal.
(35) Mimura, Y., Church, S., Ghirlando, G., Ashton, P. R., Dond, S., Goodall, M., Lund, J., and Jefferis, R. (2000) The influence of glycosylation on the thermal stability and effector function expression of human IgG1-Fc: Properties of a series of truncated glycoforms. *Mol. Immunol. 37*, 697−706.
(36) Krapp, S., Mimura, R., Jefferis, R., Huber, R., and Sondermann, P. (2003) Structural Analysis of Human IgG-Fc Glycoforms Reveals a Correlation Between Glycosylation and Structural Integrity. *J. Mol. Biol. 325*, 979−989.
(37) Ghirlando, R., Lund, J., Goodall, M., and Jefferis, R. (1999) Glycosylation of human IgG-Fc: influences on structure revealed by differential scanning micro-calorimetry. *Immunology Letters 68*, 47−52.
(38) Davis, J. M., Arakawa, T., Strickland, T. W., and Yphantis, D. A. (1987) Characterization of recombinant human erythropoietin produced in Chinese hamster ovary cells. *Biochemistry 26*, 2633−2638.
(39) Deisenhofer, J. (1981) Crystallographic refinement and atomic models of a human Fc fragment and its complex with fragment B of protein A from *Staphylococcus aureus* at 2.9- and 2.8-Å resolution. *Biochemistry 20*, 2361−2370.
(40) Lau, H., Pace, D., Yan, B., McGrath, T., Smallwood, S., Patel, K., Park, J., Park, S. S., and Latypov, R. F. (2010) Investigation of degradation processes in IgG1 monoclonal antibodies by limited proteolysis coupled with weak cation-exchange HPLC. *J. Chromatogr., B 878*, 868−876.
(41) Sahin, E., Grillo, A. D., Perkins, M. D., and Roberts, C. I. (2010) Comparative Effects of pH and Ionic Strength on Protein-Protein Interactions, Unfolding, and Aggregation for IgG1 Antibodies. *J. Pharm. Sci. 99*, 4830−4848.
(42) Thies, M. J., Talamo, F., Mayer, M., Bell, S., Ruoppolo, M., Marino, G., and Buchner, J. (2002) Folding and oxidation of the antibody domain C_H3. *J. Mol. Biol. 319*, 1267−1277.
(43) Clark, A. H., Saunderson, D. P. H., and Suggett, A. (1981) Infrared and laser-Raman spectroscopic studies of thermally-induced globular protein gels. *Int. J. Pept. Protein Res. 17*, 353−364.
(44) Casal, H. L., Köhler, U., and Mantsch, H. H. (1988) Structural and conformational changes of *β*-lactoglobulin B: An infrared spectroscopic study of the effect of pH and temperature. *Biochim. Biophys. Acta 957*, 11−20.
(45) Ismail, A. A., Mantsch, H. H., and Wong, P. T. T. (1992) Aggregation of chymotrypsinogen: Portrait by infrared spectroscopy. *Biochim. Biophys. Acta 1121*, 183−188.
(46) Dong, A., Prestrelski, S. J., Allison, S. D., and Carpenter, J. F. (1995) Infrared spectroscopic studies of lyophilization and temperature induced protein aggregation. *J. Pharm. Sci. 84*, 415−424.
(47) Byler, D. M., and Purcell, J. M. (1989) FTIR examination of the thermal denaturation and gel-formation in whey proteins. *Proceedings, 7th International Conference on Fourier Transform Spectroscopy*, Vol. *1145*, pp 415−417, SPIE, Bellingham, WA.
(48) Gokarn, Y. R., Fesinmeyer, R. M., Saluja, A., Razinkov, V., Chase, S. F., Laue, T. M., and Brems, D. N. (2011) Effective charge measurements reveal selective and preferential accumulation of anions at the protein surface in dilute salt solutions. *Protein Sci. 20*, 580−587.
(49) Saluja, A., Crampton, S., Kras, E., Fesinmeyer, R. M., Remmele, R. L., Jr., Narhi, L. O., Brems, D. N., and Gokarn, Y. R. (2009) Anion Binding Mediated Precipitation of a Peptibody. *Pharm. Res. 26*, 152−160.